PERGAMON

Journal of Structural Geology 24 (2002) 1055–1064

JOURNAL OF STRUCTURAL GEOLOGY

www.elsevier.com/locate/jstrugeo

Finite element modelling of the evolution of pressure solution cleavage

Frank Fueten[a], Pierre-Yves F. Robin[b,*], Michael Schweinberger[b]

[a]*Department of Geological Sciences, Brock University, St. Catharines, Ontario, Canada L2S 3A1*
[b]*Department of Geology, 22 Russell Street, University of Toronto, Toronto, Ontario, Canada M5S 3B1*

Received 7 December 2000; revised 18 June 2001; accepted 23 June 2001

Abstract

Deformation by 'pressure solution' (or 'water-assisted stress-induced diffusion transfer') is modelled by incorporating volume transfers — driven by variations in mean stress and competency contrast — into a finite element code for viscous deformation. The model assumes a two-component, quartz–mica mixture with a composition-dependent rheology in which the viscosity of an element is solely dependent upon the volume fraction of the mobile quartz component. Both quartz-rich and mica-rich compositions are given a high competency, with a minimum viscosity at some intermediate fraction. The model is able to reproduce many structures observed in natural tectonites: propagation and coalescence of pressure solution seams, formation of microlithons and anastomosing cleavage, and, more generally, tectonic segregation.

Keywords: Finite element modelling; Pressure solution cleavage; Viscous deformation

1. Introduction

'Pressure solution' or 'water-assisted stress-induced diffusion transfer' has been studied in rocks for more than 100 years, starting with Sorby (1863). However, many aspects of spaced cleavage formation such as the parameters that determine cleavage spacing and cleavage morphology, and the resulting rheological behaviour of a polymineralic rock deforming by pressure solution remain enigmatic. For example, experimental work has failed to reproduce spaced pressure solution cleavage. The present study models the propagation and interaction of pressure solution cleavage seams in a rock that deforms by stress-induced diffusion transfer. It is an extension of the model presented by Fueten and Robin (1992), which was based on the composition-dependent rheology proposed by Robin (1979) and was a generalisation of the *anticrack* model of Fletcher and Pollard (1981).

1.1. 'Pressure solution' and the dependence of rheological behaviour on mineral composition

The descriptions of 'pressure solution' presented by Robin (1979) and Fueten and Robin (1992) are sufficient for the present purpose. On the basis of petrographic observations, Robin (1979) proposed that the rheological behaviour of an ideal quartz–mica model rock could be accounted for by silica mobility enhanced by the presence of mica. Note that in real rocks, as discussed in Robin (1979), other minerals and chemical components are expected to take or share the same roles as those of quartz and micas in the present model. Deformation is assumed to proceed in the absence of any metamorphic reaction, and the mica component itself is assumed immobile. In such a model system, a quartz-rich rock is very competent due to the absence of catalysing micas, and a mica-rich rock is also competent because it lacks quartz to 'solve'. Hence there should be a minimum in the dependence of competency on mineral composition (Robin, 1979) such as that in Fig. 1, which illustrates the particular dependence used in this study. Fueten and Robin (1992) modelled the dependence of viscosity on the mineral composition with an expression that was easy to implement, but that had limited flexibility in the position of the minimum viscosity and in the viscosity of the mica end-member. In the present work, we explore and use a more general and more flexible relationship (see Fig. 1 and Eq. (3)). It is important to point out that the competency discussed here refers solely to a resistance of the rock to deformation by stress-induced diffusion transfer, not to a resistance to deformation by other mechanisms, such as shearing along mica-rich seams in an already layered rock. Mica-rich rocks are expected to be weak when deformation is dominated by slip along cleavage planes of the mica crystals.

* Corresponding author. Fax: +1-416-978-3938.
E-mail address: pyrobin@geology.utoronto.ca (P.-Y.F. Robin).

0191-8141/02/$ - see front matter
PII: S0191-8141(01)00091-8

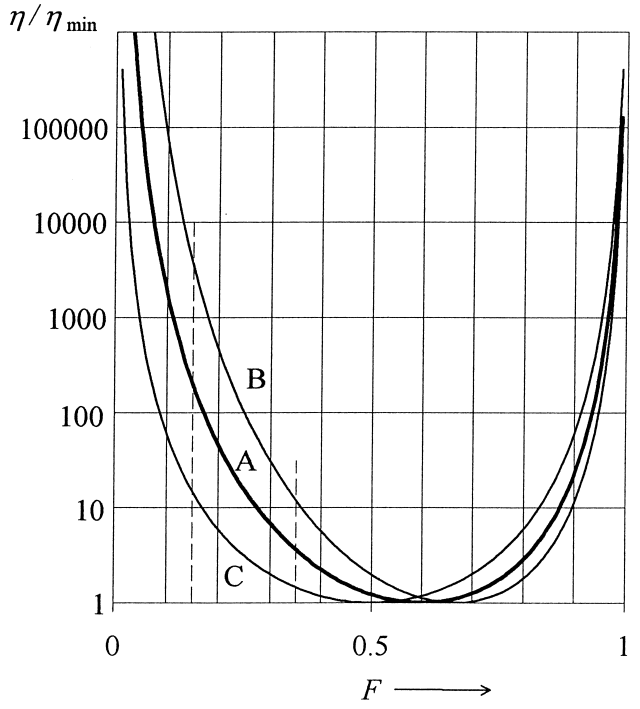

Fig. 1. Dependence of relative viscosity, η/η_{min}, on mineral fraction. The vertical dashed lines indicate the starting compositions for the bulk rock ($F = 15\%$) and for the seeds ($F = 35\%$). Curve A is that for $m = 4$ and $n = 6$ in Eq. (3), and represents the dependence used for Runs 13 and 43. When starting with our bulk composition of 15%, composition dependences described by curves such as B ($m = 4$, $n = 8$) and C ($m = 4$, $n = 4$), lead respectively, to too slow or too fast deformation.

1.2. The anticrack model, and its generalisation for penetrative 'pressure solution'

Fueten and Robin (1992) noted that Fletcher and Pollard's (1981) 'anticrack' model could be generalised by the use of the above composition-dependent rheology, thus, allowing 'pressure solution' to proceed throughout the rock, not just along a seam. They successfully modelled the propagation of one cleavage seam. Both the anticrack in an elastic medium and the pressure solutions seam in a deforming rock grow in the direction perpendicular to that of the maximum principal compressive stress. Similar to the stress concentration at the tip of the anticrack, there is a stress concentration at the tip of a cleavage seam, which is responsible for the propagation of that seam. But, whereas the deformation is everywhere elastic — except along the crack surface — in Fletcher and Pollard's anticrack, pressure solution here is penetrative. In addition, while the anticrack acquires and retains zero strength, the present pressure solution seam develops into a high strength region.

1.3. Modelling tectonic segregation

Robin (1979) argued that, assuming silica mobility and the dependence of viscosity discussed above, deformation of a quartz–mica mixture in the presence of water or other solvent is inherently unstable, in that the rock spontaneously segregates into quartz-richer and quartz-poorer domains. The present study can also be viewed as a numerical implementation of Robin's conceptual model. Other models of segregation exist. That presented by Dewers and Ortoleva (1990 and preceding ones) is the most elaborate. Its driving chemical potential gradient is that induced by mean stresses in elastic inclusions and elastic hosts; it is radically different from gradients induced by variations in normal stresses proposed by Robin (1979). The numerical model presented here does not test these alternate models.

2. Modelling pressure solution

2.1. Finite element implementation

The finite element program used here is a C implementation that runs on a SGI computer. It was modified from that used by Fueten and Robin (1992), which was itself derived from a FORTRAN program to model elastic deformation presented by Cheung and Yeo (1997). The model consists of triangular elements, each of which is assumed to be of uniform modal composition and therefore uniform viscosity, and to be under uniform stress. A mesh of 3960 triangular elements was used in all runs (see e.g. Figs. 2 and 3. This mesh is intended to represent an initial width of 10 cm, and allows for sufficiently smooth variations in parameters across the model. The model is run under plane strain.

In finite element programs, viscous flow is achieved by summing successive stress-strain increment solutions. Each iteration step calculates a strain after a time increment δt, with the succession of increments yielding the desired viscous flow. In the present study, we simulate 'closed systems', i.e. systems that can neither lose or gain silica but within which silica can diffuse freely. As in Fueten and Robin (1992), that simulation is achieved by implementing each incremental deformation iteration in two stages.

In the first stage, the finite-element solution is calculated, with each element deforming according to the two-dimensional constitutive equation:

$$\begin{bmatrix} \delta\epsilon_{xx} \\ \delta\epsilon_{zz} \\ \delta\epsilon_{xz} \end{bmatrix} = \frac{\delta t}{2\eta} \begin{bmatrix} \sigma_{xx} \\ \sigma_{zz} \\ \sigma_{xz} \end{bmatrix} \tag{1}$$

and therefore changing volume:

$$\delta\epsilon_{xx} + \delta\epsilon_{zz} = \frac{\delta t}{2\eta}(\sigma_{xx} + \sigma_{zz}) = -\frac{\delta t}{\eta}p \tag{2}$$

where normal components of stress are positive when tensile, but mean pressure, p, is positive when compressive. Pressure is generally positive and therefore, in that first stage, elements generally lose volume.

After that first stage, the areas of all the elements are summed up and, in the second stage, the entire mesh is re-inflated uniformly and isotropically so that its total area is re-established to its initial, constant value. Thus, during a given iteration, some elements lose and others gain volume. As silica from quartz is assumed to be the only mobile component, the loss or gain of volume of any element is interpreted as a loss or gain of quartz. And because the mica content of that element is fixed, its mineral composition changes, resulting in a corresponding change in its viscosity (following Fig. 1 or Eq. (3)).

It can be verified that if an element does not change volume after these two stages, its constitutive equation is the same as that for an incompressible linear viscous material (e.g. Means, 1976, Eq. 26.7). Otherwise, silica transfers among elements are in effect proportional to the differences between the value of the parameter p/η for an individual element and some space-averaged value of that parameter over the whole grid.

Although tentative and qualitative, a discussion of how the present scheme duplicates the actual chemical driving force of stress-induced diffusion transfer is in order. As already pointed out by Gibbs (1877), there can be no unique equilibrium chemical potential for the component of a solid grain under stress when that component can be mobilised along the various boundaries of that grain. This is because the equilibrium potential varies from point to point along the boundary; to a good approximation, the variations are proportional to the local compressive normal stress (Gibbs, 1877; Robin 1978). Since a finite element would have quartz boundaries in all orientations, the mean pressure, p, within a finite element could well be interpreted as providing a useful approximation of the average value for that element of the chemical potential of the mobile component. We note, however, that the actual sites of accretion of quartz within a finite element are along the boundaries under the least stress, rather than its mean stress; and that least stress has a smaller value in the elements with the highest viscosity η (Robin, 1979). Also, our interpretation of the petrographic evidence is that the amount of silica that can be mobilised from an element is a function of its mica content, and is low when the viscosity is high. These two observations concur in arguing that a higher value of its viscosity makes an element a lesser source and a better sink of silica, and therefore justify, at least qualitatively, the validity of our driving parameter p/η.

In the current modelling, the redistribution of silica over the whole grid (by the uniform re-inflation of that grid during the second stage of each iteration) amounts to assuming that silica diffusion is rapid over the size of the system but that it is limited to within that system. In other words, the size of the grid is, in effect, Fletcher's (1982) 'characteristic distance', i.e. proportional to $\sqrt{\eta D}$, where D is the diffusion constant. It would therefore be incorrect to infer that our scheme models a pressure solution process rate-limited by dissolution-precipitation: the limitation of silica transfers to the size of the grid is still mimicking diffusion as a rate-limiting step. A more sophisticated scheme could model an explicit diffusion distance, for example by assigning each element a viscosity that would depend not only on its current composition but also on the second derivative over space (calculated by finite differences) of the volume changes of elements in the previous iteration. But the calculation of finite differences would require re-meshing after each iteration step, and therefore a more sophisticated finite-element program than our present one.

2.2. Functional dependence of viscosity on composition

The mathematical relation, $\eta(F)$, chosen to model the dependence of viscosity, η, on the mica fraction, F, is characterised by a minimum viscosity, $\eta_{\min}$, for some intermediate composition, and by infinite viscosities for end members, $F = 0$ and 100%.

$$\eta = \frac{n^n m^m}{(n+m)^{n+m}} \quad \frac{1}{F^n(1-F)^m}\,\eta_{\min} \tag{3}$$

The minimum viscosity, $\eta_{\min}$, occurs for $F = n/(n+m)$. The values of m and n have no specific physical significance, but they allow us to set the position of the minimum viscosity and the upward curvature of the dependence (see Fig. 1). Three sample composition dependences, corresponding to three different (m, n) pairs, are shown in Fig. 1.

2.2.1. Choosing parameters

Following the choice of Fueten and Robin (1992), the choice of applied differential stress, $\Delta\sigma$, iteration time, δt, and of minimum viscosity, $\eta_{\min}$, were such that the strain of the weakest element in one iteration was less than 10%. In other words, the values of the stress and viscosity in any element are such that $(\Delta\sigma/2\eta)\delta t < 0.1$. It should be noted that this choice only sets a value for $(\Delta\sigma_a/2\eta_{\min})\delta t$, but does not specify the individual parameters in this ratio. In fact, because the chosen dimension of the system and the mesh size are somewhat arbitrary, the ratio itself cannot be considered to have a precise physical significance.

A number of experiments were performed, with 17 different choices of m and n, in order to find values that lead to propagation and connection between two individual cleavage seams (Fig. 2) with 1000–2000 iterations. The mineral compositions of the bulk rock and the seeds were chosen, somewhat arbitrarily, to be $F = 15$ and 35%, respectively. Given these choices, we found that when: (1) $(\eta_{15}/\eta_{\min}) > 10^3$ (e.g. Curve B in Fig. 1), no cleavage propagation occurs in 1000 iterations; and when (2) $(\eta_{15}/\eta_{\min}) < 10^2$(e.g. Curve C in Fig. 1), the mesh collapses in too few iterations. Runs presented here are for the composition dependence represented by Curve A ($m = 4, n = 6$). It should be noted that this choice is one of convenience, corresponding to our arbitrary choice of starting compositions and our number of iterations. With different input

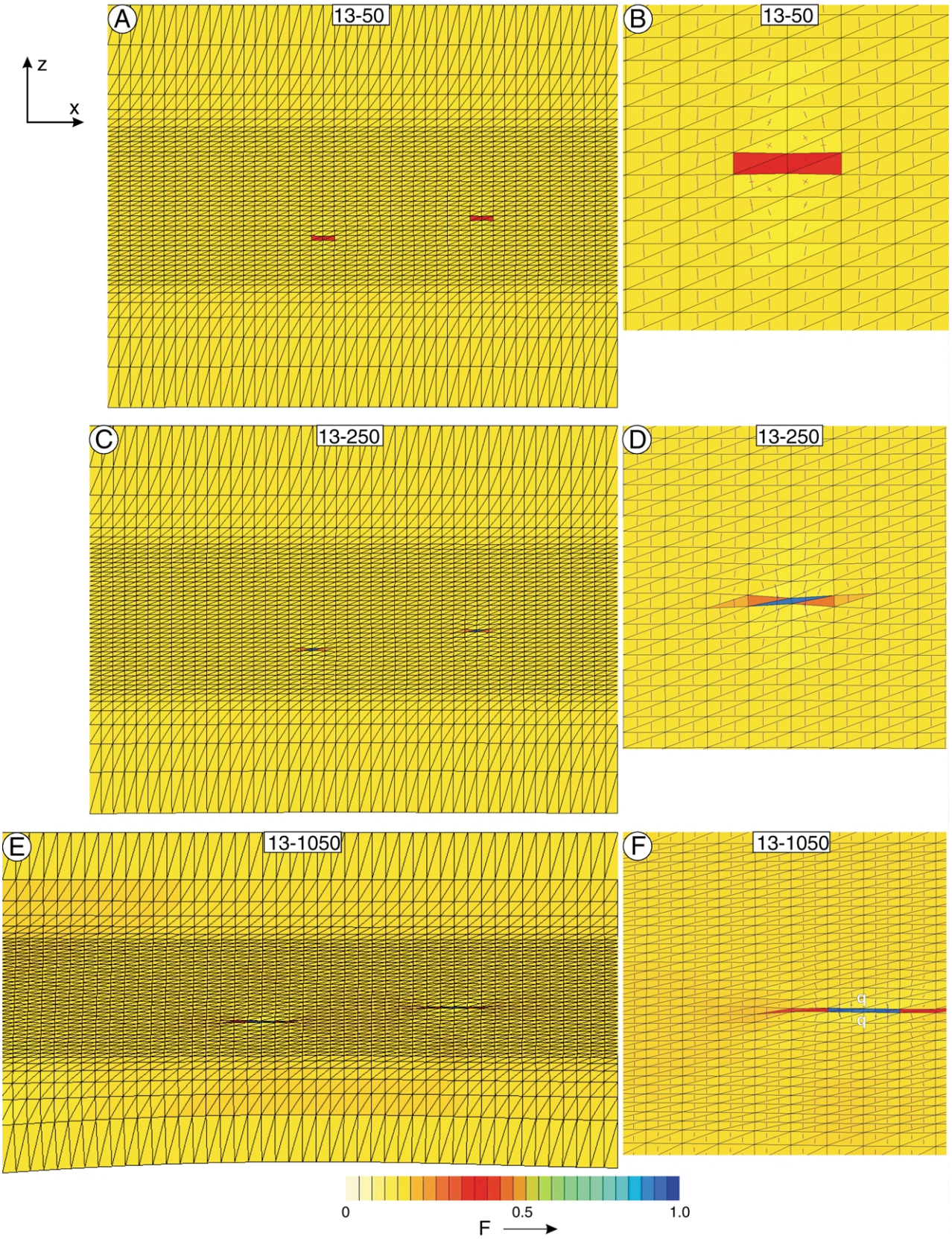

Fig. 2. Run 13: Growth and coalescence of two isolated seems. Images 13–50 to 13–1050 show the relatively isolated propagation of each seam (stage 1); 13–1400 to 13–1800 show the coalescence of the two seams (stage 2). In this and Fig. 3, the colour of an individual triangular element reflects its mineral fraction, F, according to the colour scale bar shown near the bottom of each page. The initial mica fraction of the seed elements is $F = 35\%$, that of all the other elements is 15%. The minimum viscosity is for a mica fraction of 67%, represented by a green colour. In the enlarged views shown on the right-hand sides for iterations #50 to #1500, the lines shown within each triangle give the directions and relative magnitudes of the principal stress components. In most elements, only the maximum principal compressive stress is large enough to be visible.

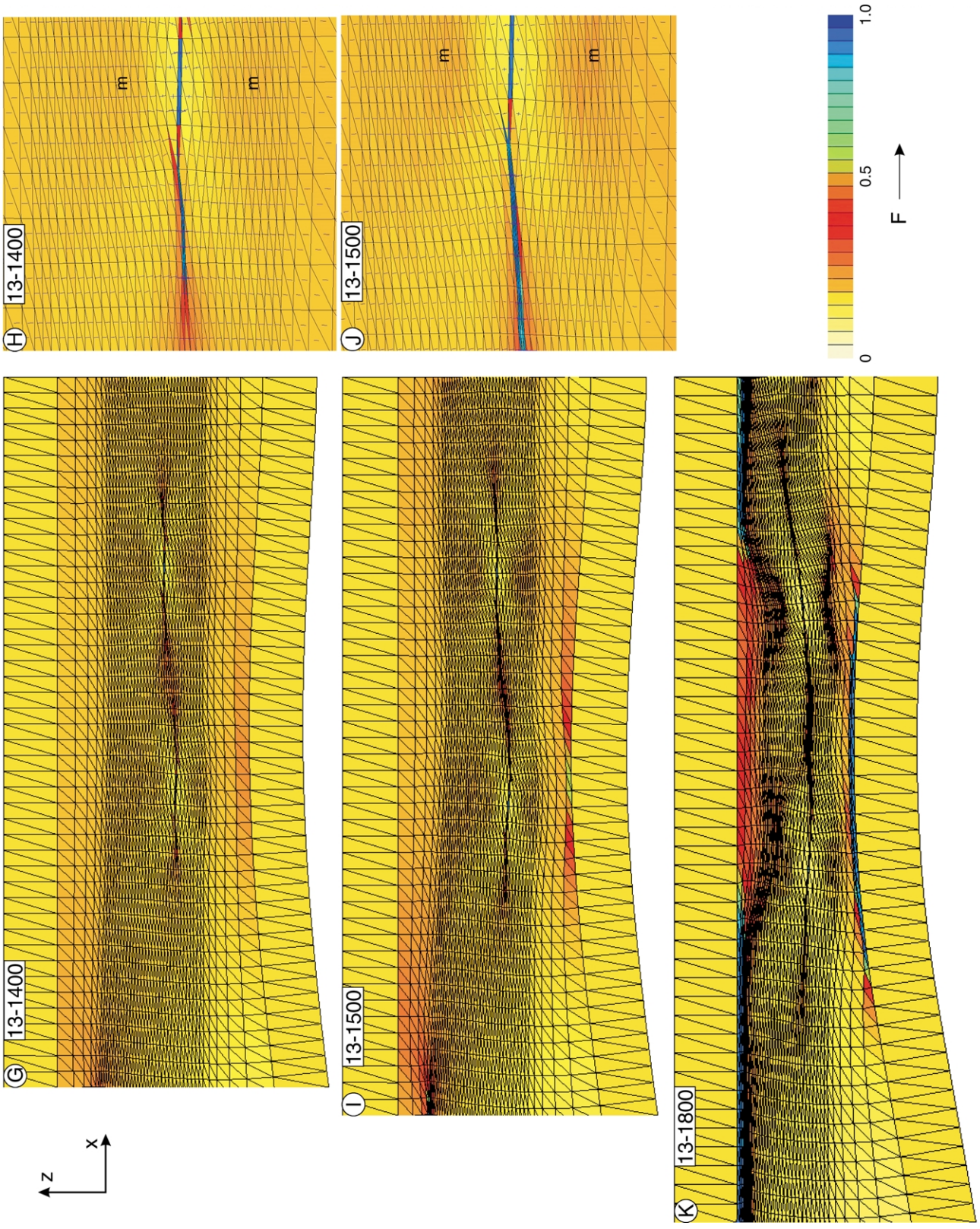

Fig. 2. (*continued*)

parameters and different run lengths, curves such as B and C might also have lead to successful runs. With this choice of m and n, the initial viscosities of the matrix and of the seeds are, respectively, $182 \times \eta_{min}$ and $3.3 \times \eta_{min}$, giving an initial ratio of matrix to seed of 55 to 1.

2.3. Boundary conditions

All nodal points along the top boundary are constrained to move only in the x-direction, whereas points along the right-boundary only move in the z-direction. In addition, the bottom left corner was constrained to only move in the z-direction in the first stage of each iteration.

A constant stress is applied along the bottom boundary. Because the centre of the mesh evolves to be weaker than the periphery, the central portion of the lower boundary bows inward in the course of the run. To counteract this tendency, the rows of largest elements along the top and bottom are assigned a fixed viscosity equal to the initial matrix viscosity of $182 \times \eta_{min}$, and therefore not allowed to weaken during the run. Because the volume of 'silica' that is lost in the first stage of an iteration is re-assigned to the whole mesh in the second stage, the top and bottom rows of elements do increase in volume; they gain silica but nevertheless preserve their fixed viscosity. Hence, although the entire mesh represents a closed system with respect to silica, the active domain, sandwiched between the two fixed-viscosity rows, does lose quartz during a run. The fixed-viscosity rows act, in effect, as silica sinks throughout the runs.

3. Results

Some 45 experiments were run to explore the evolution of cleavage seams and their interactions. We will only describe the results of two representative runs. Run 13 contains two initial seeds, and it was chosen to illustrate: (1) the growth of a single cleavage seam, and (2) the linking of two seams into a single one. Run 43 contains 18 initial seeds, and was chosen to demonstrate the development of an anastomosing pattern of cleavage seams and of microlithons to form a domainal schistosity. Observations on the textures that develop in the models are made below in the order of their evolution and illustrated in Figs. 2 and 3.

3.1. Run 13: Interaction of two cleavage seams

This run can be divided into two stages. In the first one, each seam evolves more or less in isolation. That stage provides an opportunity to review the results of Fueten and Robin (1992) for the propagation of a single seam. The interaction of two extending seams occurs during the second stage.

3.1.1. Stage 1: evolution and growth of an isolated seam, Iteration 50

Although the geometry of the elements have not changed much in the first 50 iterations, the compositions of the seed elements have already changed from the initial value of 35% mica to 36.2% for the two outer elements, and 40% for the two inner ones. Their viscosities are accordingly ca. 1/63 and 1/89, respectively, of that of the matrix. Note the deflection of the maximum principal direction of stress around the weak seam. The deflection results in a stress concentration near the edges of the seed. This deflection, already documented by Fueten and Robin (1992), is similar to the deflection of stresses around a cavity predicted by elastic theory (e.g. Jaeger, 1969, Fig. 71)

3.1.2. Iteration 250

A 'process zone' (see Fueten and Robin, 1992; Raynaud and Carrio-Schaffhauser, 1992) forms near the ends of the seed. This process zone is the result of higher strain, and consequent preferential quartz loss, due to the stress concentration; it results in a weakening of the material in front of the original seed.

The mica concentration in the central (blue) elements is 95% mica, corresponding to a viscosity that is already 20% higher than the initial viscosity of the matrix (i.e. $236 \times \eta_{min}$). The seed has therefore now become strong as a result of quartz depletion. There are now two weak regions, one at each tip, with their corresponding stress concentrations. The stress concentration on the outer side of the weak region further weakens the matrix, whereas that on the inner side, by further depleting the quartz, only strengthens the seam further.

3.1.3. Iteration 1050

The seam has propagated. Three elements on either side of the original 'seed' have reached a mica concentration $F \geqq 45\%$, three times the original concentration in the rock, which we take as definition of cleavage. The process zone is now distinctly broader and fan-shaped.

Quartz-richer zones (areas **q**, $F = 14\%$) on both walls of an initial seam are clearly visible. They had already started to form at 50 iterations, but were harder to see on the figure. Their positions, adjacent to the initially weak seed, sheltered these **q** zones from the deformation occurring elsewhere in the rock, and therefore from quartz loss. This phenomenon does not depend on the composition dependence of the rheology used; it was in fact well displayed in the earlier numerical experiments of Fueten and Robin (1992, in particular Fig. 6b–e).

Experiments show that the size of these quartz-rich zones is proportional to the size of the initial seed. Initial seeds of 16 elements (instead of four) give rise to quartz-rich zones with areas four times those observed in this image. It may be recalled here that the current modeling is scale-independent (Fueten and Robin, 1992), and does not explicitly include any characteristic diffusion distance (Fletcher, 1982).

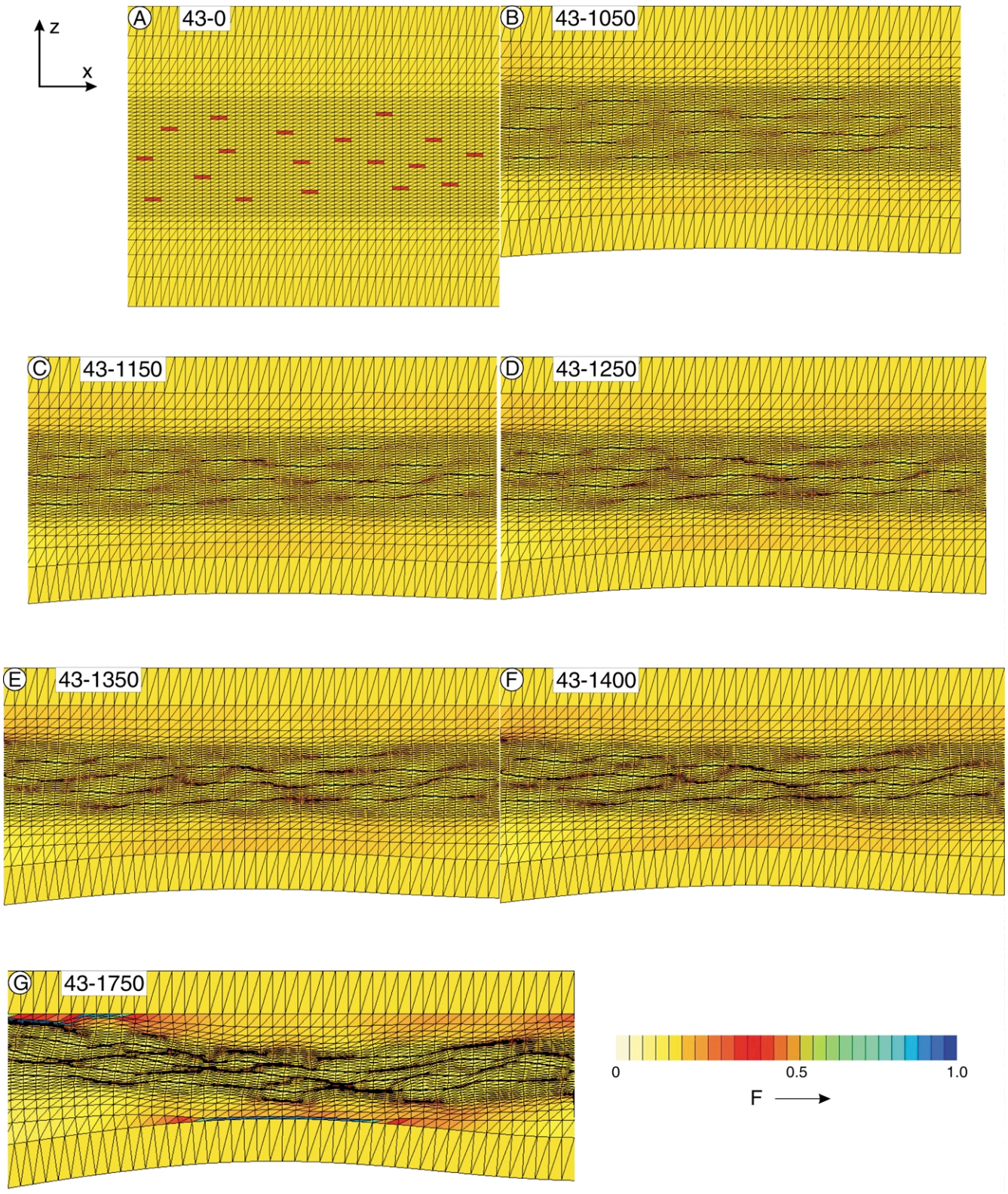

Fig. 3. Run 43: Development of a domainal schistosity — consisting of anastomosing cleavage surrounding microlithons — from 18 seeds initially scattered throughout the active area.

Some remarks concerning the development of these **q** zones are in order. Although the zones described here are better described as not having lost quartz, rather than having gained any, an actual gain in quartz by some elements is in principle possible. It should first be noted that enrichment in quartz of some domains at the expense of others is inherent to the very process of tectonic segregation, at least in a closed system: it does not violate any law of mechanics or of thermodynamics (Robin, 1979). We note also that, at the scale of individual mineral grains, any quartz gained is expected to be accreted along boundaries submitted to the least compressive normal stress (Robin, 1979). But each finite element treats the material it contains as a continuum, consisting of many grains, and therefore cannot describe the details of the quartz grain growth or dissolution processes.

The observations so far are consistent with those made by Fueten and Robin (1992) on the propagation of a single cleavage seam. There is a hint of some interaction and mutual enhancement of the two process zones facing each other: the combined size of the area of quartz depletion is greater than twice that of each outer process zone. This means that more quartz is transported away from the facing process zones than from the outer ones.

3.1.4. Stage 2: interaction and coalescence of the two seams, Iteration 1400

Each seam has propagated further. There is a strong mutual enhancement of the process zones facing each other, resulting in a greater quartz loss there than in the outer process zones. However, by our definition (elements containing more than 45% mica), the material between the seams has not yet become cleavage. The **q** zones flanking the initial seeds have caused the formation of new weak, quartz-depleted zones (areas **m**).

The lower boundary has now bowed inward, in spite of the row of strong fixed-viscosity elements. This curvature has caused quartz loss in the adjacent elements near the middle of the bow.

3.1.5. Iteration 1500

The two seams have joined into a continuous one. In fact, the new seam that formed by the collapse of the fan-shaped process zone is thicker than the initial seam: the width in the vicinity of the initial seed is fixed, constrained by the development of its quartz-rich walls. Quartz-depleted regions, **m**, are depleted further. The strain concentrations associated with the boundary conditions are now evolving into additional pressure solution seams.

3.1.6. Iteration 1800

The connecting seams continue to thicken, reaching widths of 14 elements, in contrast to widths of 6 to 10 elements in the external zones. This thickening is achieved by accretion of elements that lose almost all their quartz as they accrete. This accretion is similar to the thickening of stylolite seams by accumulations of 'insoluble' material. The **m** zones have now evolved into additional cleavage seams.

The run cannot proceed any further because the active region, that between the two fixed-viscosity rows, is now reduced to 62% of its initial volume and, because of its low average strength, is rapidly collapsing into an accumulation of mica.

3.1.7. Conclusions from Run 13

The formation of a continuous cleavage seam has been enhanced by the cooperative interaction of the two propagating process zones. This interaction is similar to that of two expanding tensile cracks. The formation of two quartz-richer zones, **q**, adjacent to, and on either side of, the initial seeds fix the width of the cleavage seam in that location, whereas the seam grows thicker elsewhere. New seams, starting as **m** zones, appear to form at set distances from the initial seeds. In our experiments, that distance is not diffusion controlled: it is proportional to the size of the initial seeds.

3.2. Run 43: Development of domainal schistosity, Iteration 0

Eighteen seeds ($F = 35\%$) are scattered within a matrix with $F = 15\%$ mica. For the first 1000 iterations, each seam evolves in isolation, in a manner similar to that described in the first stage of Run 13; the description of that evolution need not be repeated.

3.2.1. Iteration 1050

The extent of interactions between neighbouring seams is governed by overlap of their fan-shaped process-zones, which is a function of both their horizontal and vertical tip-to-tip distances. Thus some seam pairs have nearly joined while others have not interacted yet.

3.2.2. Iterations 1150 and 1250

Many more seams have joined, and **q** and **m** zones become more distinct. The cooperative interaction between process zones and adjacent **q** zones contribute to the growth of cleavage.

3.2.3. Iterations 1350 and 1400

Seams that were initially located at nearly the same horizon have now grown into continuous sub-horizontal seams. Such a continuous seam has a beaded structure: narrow where an initial seed has been flanked by **q** zones; and wide where the seam has grown from mutually enhanced process zones. The interaction between two adjacent sub-parallel seams is by coalescence of the latter, wider portions, and define regions that rapidly lose quartz. As a result, some **q** zones are now completely surrounded by mica-rich regions and take the appearance of microlithons.

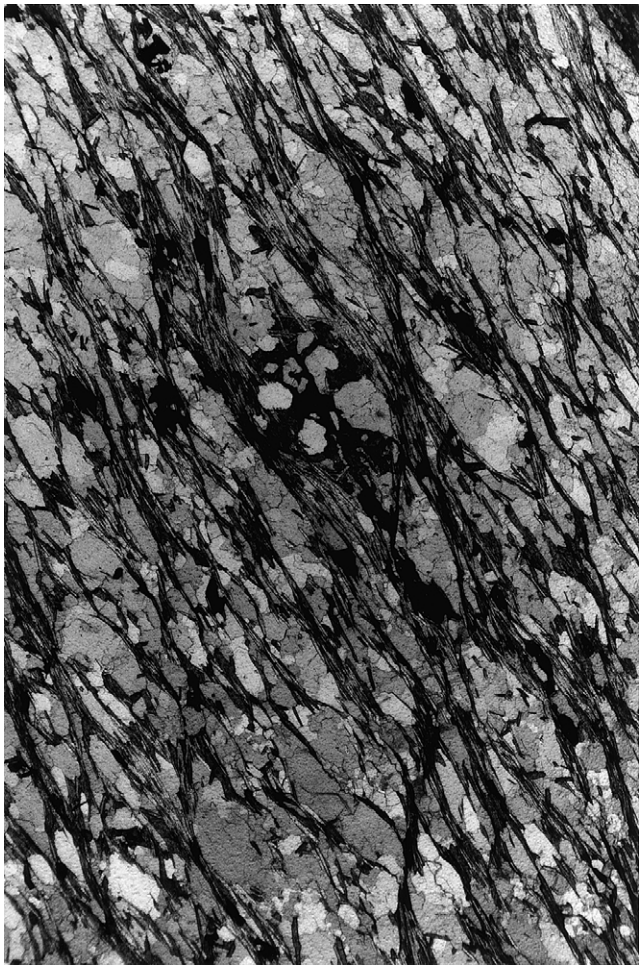

Fig. 4. Domainal schistosity in schist from Ducktown, Tennessee. Long axis of photo is 1.1 mm. Photo by W.C. Laurijssen, in Hobbs et al. (1976, Fig. 5.11a).

3.2.4. Iteration 1750

Microlithons are fully defined by an anastomosing pattern of mica seams. Some cleavage seams that were relatively straight after #1450 are now bent and deflected around microlithons. Similarly to Run 13 after the same number of iterations, the active region is now reduced to 74% of its initial volume, and about to collapse into a thick mica accumulation.

3.2.5. Conclusions from Run 43

The microlithons and the anastomosing cleavage seams develop from **q** zones that become surrounded by relatively wide process zones, which merge first along sub-horizontal seams and then coalesce with similarly wide zones in adjacent seams or with **m** zones. The combination of **q** zones and anastomosing cleavage is remarkably similar to domainal schistosity developed in slates and schists. Readers can compare this image with W.C. Laurijssen's microphotograph of domainal schistosity in schist from Ducktown, Tennessee (Fig. 4 from Hobbs et al., 1976, Fig. 5.11a), one of several examples seen in textbooks and atlases of tectonite microstructures.

4. Discussion and conclusion

4.1. Agreement between model and petrography

From petrographic evidence discussed in the introduction, Robin (1979) argued that tectonic segregation could be explained by postulating a model of deformation by stress-induced diffusion transfer — alias 'pressure solution' — that implied a composition-dependent rheology such as is shown in Fig. 1. Based on that rheology, Fueten and Robin (1992) then showed how penetrative pressure solution could be modelled using finite element viscous deformation that incorporates diffusion transfer. They applied the method to demonstrate the propagation of a single cleavage seam. In the present work, more extensive and complex textures can be observed to arise. The model is able to reproduce many features of real spaced cleavage: cleavage growth, anastomosing cleavage seams, microlithons, and fan-shaped process zones. We take the above agreement between model predictions and petrographic observations as supporting the validity of the model assumptions as well as that of the use of our two-stage iteration steps to model pressure solution with finite elements. That this simple model is able to produce realistic cleavages, without the need for crenulations or any other special requirements, suggests that the process of cleavage formation can indeed simply result from a rheological instability. This may explain why it is such a common geological feature. Robin (1979) has discussed possible relationships between tectonic segregation with and without crenulation and has argued that there should be a continuum between the two.

4.2. Tectonic segregation, ***q*** and ***m*** zones, and the quasi-periodicity of tectonic foliation

In a more general way, the present finite element modelling can be seen as a two-dimensional implementation of the schematic and conceptual one-dimensional model of tectonic segregation proposed by Robin (1979). The runs also give us a hint of what may be operating in the development of the quasi periodicity of some tectonic segregation and 'pressure solution' cleavages. Because an initiating cleavage seam protects the rock that flanks it on either side from early deformation, this protected rock — zones **q** — gains quartz compared with the surrounding matrix, and accordingly becomes stronger. That relative strength, in turn, imposes additional deformation in adjacent zones **m**, which translates into a relatively more important quartz loss there. These **m** zones can then evolve into new cleavage seams, echoing, at set distances from it, the seam that started them. It is important to recall again that in this work, as in Fueten and Robin (1992), diffusivity of silica is not

modelled specifically. The size of the grid is, in effect, the diffusion range, and the silica lost by an element is as likely to be relocated to the far end of the grid as to a nearby element. In the present modelling therefore, the distance between an initial seam and its echoing **m** zones is only set by the size of the seed that is put in to trigger the instability: it is not set by some intrinsic diffusive property of the rock. In modelling that would incorporate diffusion explicitly, the size of the **q** zones would presumably be related to Fletcher's (1982) 'characteristic distance' discussed above. But the strengthening of these **q** zones and the corresponding induced weakening of **m** zones would proceed as in the present modelling. The spatial periodicity of the cleavage would then be proportional to the 'characteristic distance'.

Acknowledgements

This research was supported by Canadian National Science and Engineering Research Grants to FF and PYFR. The authors are grateful to David Ball, Andreas Paulish, and Scott Goodchild for their work on successive versions of the finite element program, to Sigmar Stiasny for some initial experiments, to Mike Lozon for work on Figs. 2 and 3, and to Russ Pell Pysklywec and Blair Hrabi for their useful comments on an early version of the manuscript. Michael L. Williams, Nick Beeler, and Alison Ord are thanked for providing thoughtful reviews. The authors also thank Paul Williams for providing the photograph for Fig. 4 and to Bruce Hobbs, Win Means and Paul Williams for granting us its use.

References

Cheung, F.K., Yeo, M.F., 1979. A Practical Introduction to Finite Element Analysis. Pitman, London.

Dewers, T., Ortoleva, P., 1990. Geochemical self-organization III: a mechano–chemical model of metamorphic differentiation. American Journal of Science 290, 473–521.

Fletcher, R.C., 1982. Coupling of diffusional mass transport and deformation in a tight rock. Tectonophysics 83, 275–291.

Fletcher, R.C., Pollard, D.D., 1981. Anticrack model for pressure solution surfaces. Geology 9, 419–424.

Fueten, F., Robin, P.-Y.F., 1992. Finite element modelling of the propagation of a pressure solution cleavage seam. J. Structural Geology 14, 953–962.

Gibbs, J.W., 1877. On the equilibrium of heterogenous substances — the conditions of internal and external equilibrium for solids in contact with fluids with regard to all possible states of strain of the solids. Trans. Conneticut Acad. 3, 343–379.

Hobbs, B.E., Means, W.D., Williams, P.F., 1976. An Outline of Structural Geology. John Wiley & Sons, New York.

Jaeger, J.C., 1962. Elasticity, Fracture and Flow. Methuen, London.

Means, W.D., 1976. Stress and Stain. Basic Concepts of Continuum Mechanics for Geologists. Springer, New York.

Raynaud, S., Carrio-Schaffhauser, E., 1992. Rock matrix structures in a zone influenced by a stylolite. J. Structural Geology 14, 973–980.

Robin, P.-Y.F., 1978. Pressure solution at grain-to-grain contacts. Geochimica Cosmochimica Acta 42, 1383–1390.

Robin, P.-Y.F., 1979. Theory of metamorphic segregation and related processes. Geochimica Cosmochimica Acta 43, 1587–1600.

Sorby, H.C., 1863. Über Kalkstein Geschiebe mit Eindrücken. Neues Jb. Miner. 34, 801–807.